Magna Scientia Advanced Research and Reviews
eISSN: 2582-9394
Cross Ref DOI: 10.30574/msarr
Journal homepage: https://msarr.magnascientiapub.com/

(RESEARCH ARTICLE)

Check for updates

INTEGRATING COMMINUTION TESTWORK INTO GEOMETALLURGICAL RECOVERY FRAMEWORKS: A CRITICAL REVIEW OF SPATIAL HARDNESS MODELLING FOR U.S. CRITICAL MINERAL OPERATIONS

Pierre Mensah *

Independent Mining Researcher, Hancock, Michigan, USA.
* Corresponding Author

Magna Scientia Advanced Research and Review, 2026, 18(01), 261–269

Publication history: Received on 14 September 2026; revised on 22 October 2026; accepted on 24 October 2026

Article DOI: https://doi.org/10.30574/msarr.2026.18.1.0214

Copyright © 2026Author(s) retain the copyright of this article. This article is published under the terms of the Creative Commons Attribution License 4.0

ABSTRACT

Variability in ore hardness drives much of the gap between predicted and actual mill throughput, and accounts for a substantial share of downstream recovery shortfalls in critical mineral operations. Even so, many U.S. feasibility studies still treat hardness as a single average value across the deposit. The Bond Work Index (BWi) is still the industry's default for grindability, but the test consumes about 10 kg of sample and takes about eight hours per determination, which keeps the number of determinations low at the resource-estimation stage. This paper pulls together recent peer-reviewed work on three connected questions: How can a comminution testwork programme capture spatial variability without running thousands of BWi determinations? How can hardness domains be modelled in space once that data is in hand? And how do those domains feed into a geometallurgical recovery framework? The proxy methods reviewed include the point load index, Leeb rebound hardness, the Cerchar abrasivity index, and hyperspectral imaging. The throughput-prediction case study draws on operating SAG mill circuits, and the closing section ties the methodological picture to federal supply chain assessments under the 2025 List of Critical Minerals and Executive Order 14241.

Keywords: Bond Work Index; Comminution; Geometallurgy; Spatial Hardness; Throughput Prediction; Critical Minerals; SAG Mill; Hyperspectral Imaging; Point Load Index

1 INTRODUCTION

A processing plant meets its production targets when two linked predictions are correct: how much energy each tonne of ore will consume in the mill, and how much tonnage the mill can therefore handle per hour. Both predictions depend on knowing how hardness varies across the deposit. In current geometallurgical practice, this hardness variation is mainly tracked using the Bond Work Index, or BWi. The BWi value is assigned block by block across the mineable volume of the deposit. The standard Bond ball mill grindability test, however, needs about 10 kg of sample, takes between four and eight hours per determination, and is restricted to a specific feed particle size distribution that often does not match actual mill feed (Nikolić et al., 2025). Because of these constraints, feasibility-stage programmes usually include only a handful of BWi determinations spread across a deposit , which has pushed researchers toward faster, cheaper proxies (Ghadernejad et al., 2026).

The policy context for this work has shifted noticeably in the last year. Executive Order 14241, signed on 20 March 2025 (Federal Register, 90 FR 13673), calls for immediate measures to increase domestic mineral production on national security grounds (White House, 2025). The final 2025 List of Critical Minerals followed on 7 November 2025 (Federal Register, 90 FR 50494) and names sixty commodities of supply chain concern, among them lithium, cobalt, copper, nickel, and sixteen individual rare earth elements (USGS, 2025b). The supply risk methodology that sits behind the List is set out in USGS Open-File Report 2025-1047 (Nassar et al., 2025). Together, these instruments give operators a strong incentive to produce accurate, low-cost geometallurgical characterization of U.S. critical mineral deposits.

The principal U.S. critical mineral deposit types each present a different comminution problem. Spodumene-hosted lithium pegmatites show recovery variability that is driven by the close mineralogical association between spodumene and gangue phases such as feldspar, quartz, and muscovite (Sahoo et al., 2024). Reagent chemistry, surface properties, and water quality have all been documented as critical factors in spodumene flotation efficiency (Tadesse et al., 2024). Mountain Pass in California is the only operating U.S. REE producer. USGS reporting for 2024 puts ore throughput at 576,376 t at an average head grade of 8.55% TREO, with bastnaesite concentrate grading 61.0% TREO and an overall TREO recovery of 69.1% (USGS, 2025a). The bulk of domestic copper still comes from porphyry deposits in Arizona, Utah, and New Mexico;

The rest of the paper is organised as follows. Section 2 looks at the geological reasons hardness varies differently in each of these deposit types. Section 3 turns to the laboratory side, working through the standard Bond test alongside the principal proxy methods. Section 4 deals with how those measurements are extended in space, and Section 5 with how well the resulting predictions hold up against operating throughput. Section 6 connects all of this back to U.S. supply chain assessments, and Section 7 concludes.

2 GEOLOGICAL DRIVERS OF HARDNESS VARIABILITY IN U.S. CRITICAL MINERAL DEPOSITS

The hardness of any given ore depends on which minerals are present , how those minerals are arranged in the rock, and how much weathering has worked on the deposit. Each of the main U.S. critical mineral deposit types brings these three factors together in a different way, and that combination shapes which testwork programme is appropriate for the deposit.

2.1 Spodumene Pegmatite Systems

Hard-rock lithium production in the United States is built around spodumene pegmatites, which sit at the center of several domestic supply initiatives. Beneficiation flowsheets typically combine some mix of dense-medium separation, magnetic separation, and froth flotation, with the exact configuration depending on liberation size and the suite of gangue minerals present (Sahoo et al., 2024). From a comminution standpoint, the difficulty lies in how closely spodumene intergrows with feldspar, quartz, and muscovite. These gangue minerals share enough surface chemistry with spodumene to make flotation selectivity awkward, so grind size must be tuned carefully, too coarse and liberation suffers, too fine and grinding energy climbs without much further benefit. Reagent chemistry, surface conditioning, and water quality also matter (Tadesse et al., 2024). At pilot scale, Wang et al. (2025) recently reported Li_2O concentrate grades of 5.80% at 88.62% recovery using a comprehensive utilization flowsheet.

2.2 Cobalt and Nickel Deposits

U.S. cobalt resources sit in two quite different geological settings. The first is the Blackbird district in east-central Idaho, where cobalt occurs mainly as cobaltite (CoAsS) accompanied by chalcopyrite and minor accessory phases in metasedimentary host rocks (USGS, 2025a); the processing route relies on selective sulfarsenide flotation. The second is the Eagle Mine in Michigan, a Proterozoic magmatic nickel-copper sulfide system in which cobalt sits in pentlandite and pyrrhotite (USGS, 2025a). For these magmatic Ni-Cu sulfide ores, the level of comminution variability tracks how well pentlandite grains are liberated, which is itself controlled by igneous texture: disseminated sulfide zones need finer grinding than massive sulfide zones. Both cobalt and nickel appear on the 2025 List of Critical Minerals (USGS, 2025b).

2.3 Rare Earth Element Deposits

Sixteen individual rare earth elements appear on the 2025 List: cerium, dysprosium, erbium, europium, gadolinium, holmium, lanthanum, lutetium, neodymium, praseodymium, samarium, scandium, terbium, thulium, ytterbium, and yttrium (USGS, 2025b). Of all the commodities on the List, REEs are among those whose disruption federal supply chain analysis rates as carrying the highest economic cost (Nassar et al., 2025). The only operating U.S. producer is the Mountain Pass carbonatite deposit in California. The comminution challenge for REE carbonatites is that recovery is not really controlled by total REE grade. It is controlled by how the REEs are distributed across mineral phases: bastnäsite-hosted REE recovers efficiently in gravity-flotation circuits, while monazite-hosted REE needs a different reagent suite and ends up at lower recovery. A routine geochemical assay returns a total REE number but says nothing about how

those REE are partitioned among minerals, which is why operators at Mountain Pass have turned to hyperspectral imaging to fill in that picture (Adidam et al., 2024).

2.4 Copper Porphyry Deposits

Porphyry copper deposits in Arizona, Utah, and New Mexico account for most U.S. copper supply, and copper itself was added to the 2025 List of Critical Minerals (USGS, 2025b). Hardness in these systems shifts vertically with the sulfide–transitional–oxide zonation, and the appearance of secondary copper minerals such as malachite and chrysocolla in the oxide cap changes both grinding behavior and downstream metallurgy. Working on a copper porphyry deposit in Espinar (Cusco, Peru), Vargas et al. (2025) compared throughput-prediction models built on 174 JK Drop Weight Tests, 1,172 BWi tests, and three years of operating data, and reached mean relative deviations of around 1.5%. Volcanogenic massive sulfide systems are much smaller in tonnage but bring their own comminution headaches (Goodall et al., 2025).

3 COMMINUTION TESTWORK METHODOLOGIES: CRITICAL EVALUATION

3.1 The Bond Ball Mill Work Index

More than seventy years after Bond (1952) standardized it, the Bond ball mill work index test is still the test most operations reach for when a single grindability number is needed. Bond's third theory of comminution writes the specific energy required for size reduction as:

$$W = W_i\left(\frac{10}{\sqrt{P_{80}}} - \frac{10}{\sqrt{F_{80}}}\right) \tag{1}$$

with W as the specific energy input (kWh/t), W_i the Bond Work Index (kWh/t), and P_{80} and F_{80} the 80% passing sizes of product and feed respectively (μm). Running the test takes roughly 10 kg of sample, a standard ball charge in a 305 mm × 305 mm mill, and several hours of locked-cycle grinding per determination (Nikolić et al., 2025). Sample mass and time are obvious constraints, although there are others. The procedure assumes the feed already passes 3.35 mm; when it does not, correction factors have to be applied, and Nikolić et al. (2025) point out that these corrections introduce additional uncertainty of their own.

3.2 The Point Load Index as a BWi Proxy

Unlike the Bond test, the point load strength index ($I_{s(50)}$) can be run on small core pieces or even irregular rock fragments in the field, takes minutes rather than hours, and costs almost nothing per determination, exactly the combination needed for high spatial density. The corrected index for a standard 50 mm diameter specimen is computed as:

$$I_{s(50)} = \frac{F}{D_e^2}, \qquad D_e = \sqrt{\frac{4\,A_{min}}{\pi}} \tag{2}$$

with F the failure load, D_e the equivalent diameter, and A_{min} the minimum cross-sectional area at failure. Jamshidi and Sousa (2024) examine how well PLI predicts uniaxial compressive strength relative to Brazilian tensile strength, and their comparison gives the empirical grounding for using PLI as a high-density proxy for the mechanical properties that drive comminution behavior. For irregular specimens, Zhang et al. (2025) propose an equivalent area method that reduces measurement bias compared with the older loading-span and equivalent-diameter conventions. None of this means PLI translates directly into BWi: the relationship is deposit-specific and has to be calibrated against laboratory BWi determinations on co-located samples. Once that calibration is in hand, however, PLI works well as a dense complement to the limited BWi testwork that is feasible at resource stage.

3.3 Hyperspectral Imaging and Multi-Proxy Frameworks

Hyperspectral core scanning gives continuous, non-destructive mineralogical information across drill core at 1–5 mm per pixel in the visible-near infrared and shortwave infrared ranges. Because BWi is tied to mineralogy in the first place, that imagery can feed directly into machine-learning models built to predict hardness. Ghadernejad et al. (2026) worked with 62 hand-size rock samples drawn from two adjacent Canadian open-pit gold mines and showed that Leeb rebound hardness (LRH) and Cerchar abrasivity index (CAI) cleanly separate hard (>15 kWh/t BWi) from moderate (<15 kWh/t BWi) grindability classes, while features pulled from hyperspectral imaging and pXRF added complementary predictive power. Their random forest regressors predicted LRH and CAI with R^2 of 0.74 and 0.79 respectively (Figure 1), drawing mostly on SWIR-region spectral features identified by an automated band-ratio pipeline.

Figure 1 plots the random forest regressor R^2 values from Ghadernejad et al. (2026) for HSI-based prediction of two rock hardness proxies on their Canadian gold-ore dataset. Both proxies clear the practical deployment threshold of R^2 = 0.70, which suggests HSI-driven high-density hardness characterization can usefully complement laboratory BWi testing.

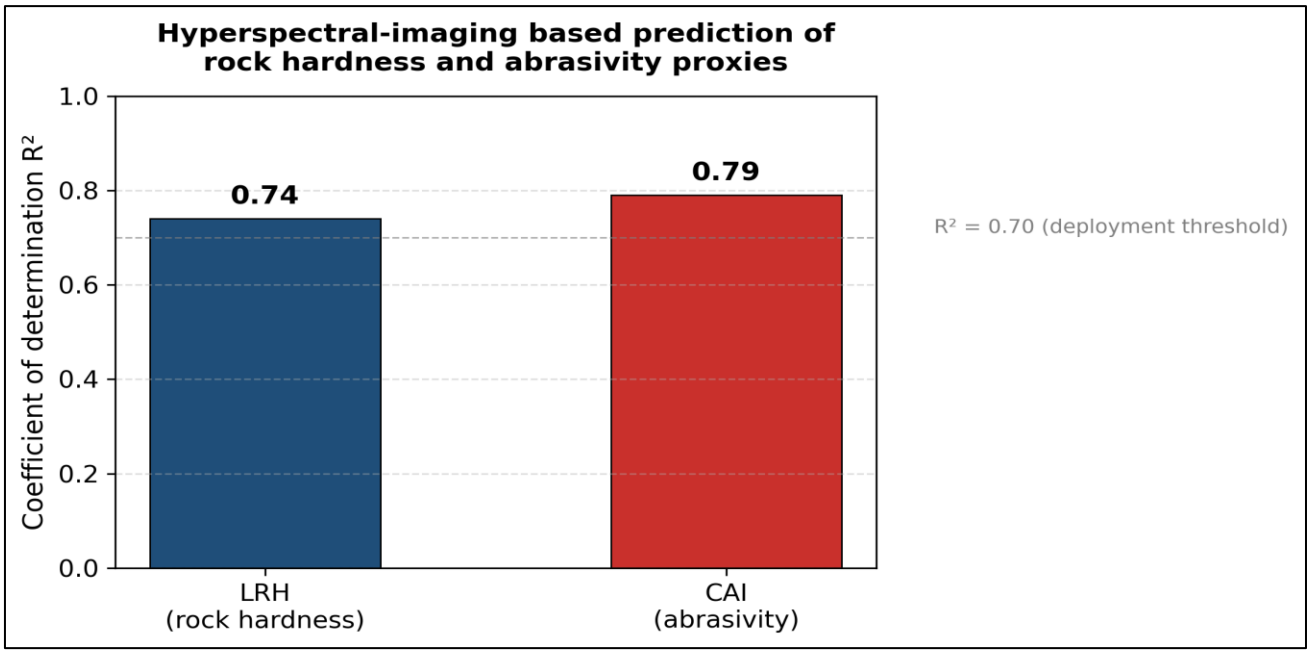


Figure 1: Random forest regressor R^2 values for hyperspectral-imaging based prediction of Leeb rebound hardness (LRH) and Cerchar abrasivity index (CAI) on 62 hand-size rock samples from two adjacent Canadian open-pit gold mines.

Source: Data extracted from Ghadernejad, S., Abdolmaleki, M., & Esmaeili, K. (2026). A multi-proxy framework for predicting ore grindability: Insights from geomechanical and hyperspectral measurements. Minerals, 16(1), 115. https://doi.org/10.3390/min16010115. Figure prepared by the author from values reported in the paper's abstract and results section.

A general empirical proxy regression takes the form:

$$\widehat{W}_i = \alpha_0 + \sum_{k=1}^{K} \alpha_k \, x_k + \varepsilon \tag{3}$$

where $\hat{W}_i$ is the predicted Bond Work Index, x_k are predictor variables (PLI, LRH, CAI, mineralogical fractions, geochemical indices), α_k are estimated regression coefficients, and ε is residual error. For non-linear, high-dimensional predictor relationships, ensemble tree-based methods such as random forest tend to outperform linear regression. The random forest prediction at point x is the average across the ensemble:

$$\hat{y}(x) = \frac{1}{T}\sum_{t=1}^{T} f_t(x) \tag{4}$$

with T the number of trees and $f_t(x)$ the prediction of the t-th tree, each grown on a bootstrap re-sample of the training set. In the Ghadernejad et al. (2026) model, the most important features sat mainly in the SWIR window (1000–2500 nm), which lines up with where clay minerals and alteration assemblages, the phases that largely dictate rock mechanical behavior , produce their distinctive absorptions.

4 SPATIAL MODELLING OF COMMINUTION HARDNESS DOMAINS

Spatial hardness modelling tends to fall into one of two camps. The first carves the deposit into geological domains, defined from logging and analytical data, and assigns a representative BWi to each block within a domain. The second skips the domain boundaries altogether, treating BWi as a continuous spatial variable that can be kriged or simulated across the whole deposit. Adusei-Gyamfi et al. (2024), in a review of uncertainty in resource estimation, summarize the trade-off well: the domain approach is easy to follow and easy to explain but only as good as the domain interpretation,

while the continuous approach is more objective on its own terms but tends to smear hardness across lithological contacts where it shouldn't.

Hybrid approaches that combine geostatistics with machine learning have become something of a default for spatial modelling of geological and metallurgical variables. Dutta and Emery (2024) work through a tandem framework in which random forests handle rock-type classification and geostatistics simulate within-domain values, and the same architecture transfers cleanly to spatial hardness modelling. Riquelme (2025) takes this further with a dual random field framework that is built for exactly the situation operators face most often: dense sampling of input variables, sparse sampling of the response outcomes, explicitly naming metallurgical recovery and mining throughput as the kinds of responses it is meant for. Mehrali (2026) goes one step further, pairing multivariate geostatistical simulation with ensemble Kalman filter updating so that block model realizations can be adjusted sequentially as production data come in.

For variogram-based kriging of BWi, Wang (2024) reviews the broader uncertainty-quantification picture in geochemical mapping and shows that simple kriging substantially smooths the underlying variability of geochemical fields. That smoothing is particularly awkward for hardness models, because the practical consequence of under-modelled local variability is throughput under-prediction during periods of harder-than-average mill feed. Hoerger and Dagdelen (2025), reviewing stochastic production scheduling, describe how conditional simulation gets around this by drawing ensembles of realizations that preserve the modelled variability instead of averaging it away.

5 THROUGHPUT PREDICTION PERFORMANCE ON OPERATING COMMINUTION CIRCUITS

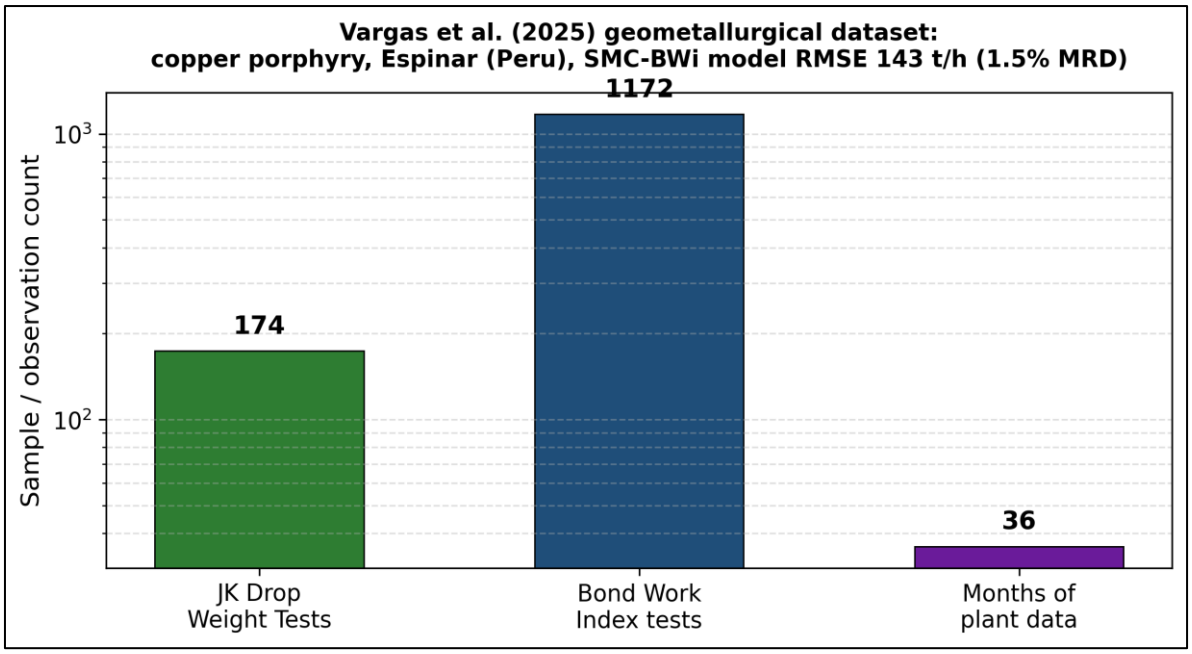


Figure 2: Composition of the verified geometallurgical dataset from Vargas et al. (2025) on a copper porphyry deposit in Espinar (Cusco, Peru). The best performing model (SMC-BWi) achieved RMSE 143 t/h and mean relative deviation 1.5% against actual plant throughput.

Source: Data extracted from Vargas, F., Pinedo, V., Quiroz, M., & Vásquez, F. (2025). Comparative analysis of throughput prediction models in SAG mill circuits: A geometallurgical approach. Mining, 5(3), 37. *https://doi.org/10.3390/mining503003* . Figure prepared by the author from values reported in the paper's abstract and methodology section.

The real test of any hardness model is whether it predicts mill throughput well enough to be useful, and on that question the benchmark of Vargas et al. (2025) is the most thorough recent example. Working on a copper porphyry in Espinar (Cusco, Peru), the authors compared three model formulations (DWi-BWi, SGI-BWi, and SMC-BWi). The underlying dataset, summarized in Figure 2, contains 174 JK Drop Weight Tests, 1,172 Bond Work Index determinations, and 36 months of plant operating data. Pairing SMC parameters with BWi gave the best result: an RMSE of 143 t/h and a mean relative deviation of 1.5% against actual throughput. That accuracy did not come cheaply, it rested on more than 1,300 laboratory tests in total and three years of careful reconciliation against operating data.

Figure 2 shows the scale of the Vargas et al. (2025) dataset behind that throughput benchmark on a copper porphyry SAG mill circuit.

Model performance here is reported through the coefficient of determination

$$R^2 = 1 - \frac{\sum_i (y_i - \hat{y}_i)^2}{\sum_i (y_i - \bar{y})^2} \tag{5}$$

with y_i the observed plant throughput in reconciliation interval (where i indexes the reconciliation intervals from 1 to N) , $\hat{y}_i$ the model prediction for that interval, $\bar{y}$, the mean of the observations, and N the total number of intervals. Alongside R^2, Vargas et al. (2025) report the mean relative deviation:

$$\text{MRD} = \frac{1}{N} \sum_{i=1}^{N} \left| \frac{\hat{T}_i - T_i}{T_i} \right| \tag{6}$$

with T_i and $\hat{T}_i$ the observed and predicted throughput in interval i. The 1.5% MRD reported by Vargas et al. sets a useful upper bar for what can be done on a well-instrumented operating SAG mill when both the laboratory and reconciliation work are taken seriously.

A related contribution comes from Kabemba and Waters (2025), working on a platinum group element orebody in the Northern Limb of the Bushveld igneous complex. They use regression-based machine learning to predict BWi from measured mineralogical descriptors, then feed those predictions into a particle swarm optimization that searches for blending strategies to keep mill performance on target. The case study itself is South African, but the overall architecture, predict a process-relevant property from mineralogy with ML, then optimize blending around it, carries over directly to U.S. critical mineral operations. Davies et al. (2025) and Fu et al. (2025) survey the wider mineral-geosciences ML literature; both point to data quality, consistent sampling, and weak interdisciplinary integration as the things that decide whether an ML method makes it from a paper into a plant.

Table 1 compares the principal testwork methods discussed so far in this paper.

Table 1: Comparative Characteristics of Comminution Testwork Methods

Method	Output	Sample requirement	Spatial density achievable	Indicative reference
Bond Ball Mill	BWi (kWh/t)	~10 kg, standard PSD	Low (domain composites)	Nikolić et al., 2025
Point Load Index	Is(50) (MPa)	~0.05 kg per test	Very high (per metre of core)	Jamshidi & Sousa, 2024; Zhang et al., 2025
Leeb Rebound Hardness	LRH (HLD)	Hand specimen or core surface	High (non-destructive)	Ghadernejad et al., 2026
Cerchar Abrasivity	CAI	Polished rock surface	Moderate	Ghadernejad et al., 2026
Hyperspectral Imaging	Mineralogical features	Drill core (non-destructive)	Continuous (1–5 mm pixels)	Ghadernejad et al., 2026
JK Drop Weight Test	A×b, ta parameters	~50 kg per test	Very low	Vargas et al., 2025
SMC Test	DWi, Mia, Mib	~25 kg per test	Low	Vargas et al., 2025

Source: Author's synthesis from the cited references. BWi = Bond Work Index; Is(50) = corrected point load index at 50 mm equivalent diameter; HLD = Leeb hardness scale (D-type impact device); CAI = Cerchar Abrasivity Index; PSD = particle size distribution.

Table 2 collects the headline performance numbers from the case studies cited above.

Table 2: Headline Performance Numbers from the Case Studies Reviewed

Study	Commodity / context	Method / output	Reported value
Vargas et al. (2025)	Copper porphyry, Peru (174 JKDWT; 1,172 BWi; 36 mo plant data)	SMC-BWi geometallurgical model RMSE	143 t/h (MRD 1.5%)
Ghadernejad et al. (2026)	Gold ore, Canada (62 samples, 10 ore groups)	HSI → LRH random forest R^2	0.74
Ghadernejad et al. (2026)	Gold ore, Canada (62 samples, 10 ore groups)	HSI → CAI random forest R^2	0.79
Wang et al. (2025)	Lithium pegmatite, pilot scale	Li_2O concentrate grade / recovery	5.80% / 88.62%
USGS (2025a)	Mountain Pass (US REE), 2024 operating data	TREO recovery / concentrate grade	69.1% / 61.0% TREO

Source: All values are reproduced verbatim from the cited primary sources. JKDWT = JK Drop Weight Test; BWi = Bond Work Index; MRD = mean relative deviation; HSI = hyperspectral imaging; LRH = Leeb rebound hardness; CAI = Cerchar abrasivity index; TREO = total rare earth oxide.

6 IMPLICATIONS FOR U.S. CRITICAL MINERAL SUPPLY CHAIN ASSESSMENTS

Executive Order 14241 (White House, 2025) and the 2025 List of Critical Minerals (USGS, 2025b) only mean something at the policy level if the underlying domestic production projections are credible , and those projections depend on recoverable reserve estimates that already bake in assumptions about recovery and throughput. Those assumptions, in turn, are only as good as the comminution work that sits behind them. Nassar et al. (2025) supply the economic machinery that turns these inputs into expected GDP impacts under disruption scenarios. Better hardness characterization, of the kind made possible by the proxy methods in Ghadernejad et al. (2026), Jamshidi and Sousa (2024), and Zhang et al. (2025), together with the integrated modelling frameworks reviewed by Adusei-Gyamfi et al. (2024) and Davies et al. (2025), therefore matters for national supply chain credibility, not just for individual mine economics.

For operators developing U.S. critical mineral projects, three practical steps follow from the review above. First, supplement the limited BWi testwork that is feasible at the resource stage with high-density proxy data: PLI on all available core, plus LRH and hyperspectral imaging on representative intervals. Second, calibrate the proxy-to-BWi relationship using paired measurements at a density that matches the geological complexity of the deposit, following the workflow set out in Ghadernejad et al. (2026). Third, when proxy-derived BWi values feed into the resource block model, report cross-validated prediction performance using the metrics in Equations (5) and (6) rather than just point estimates. On the regulatory side, the federal agencies that maintain the Nassar et al. (2025) supply risk methodology could go further and require operating mines to disclose their throughput reconciliation performance. That would let national supply projections be calibrated against what plants actually deliver, rather than against feasibility-study assumptions.

7 CONCLUSIONS

This paper has worked through the methodological landscape for comminution characterization in U.S. critical mineral operations. The standard Bond ball mill grindability test is still the workhorse measure of ore grindability, but sample mass and test duration cap the spatial density that any feasibility-stage programme can realistically achieve. Recent peer-reviewed work on proxy methods , point load index (Jamshidi & Sousa, 2024; Zhang et al., 2025), Leeb rebound hardness and Cerchar abrasivity index (Ghadernejad et al., 2026), and hyperspectral imaging coupled with machine-learning interpretation (Ghadernejad et al., 2026) , opens up a credible path to higher-density spatial hardness characterization, with reported R^2 values of 0.74 and 0.79 for HSI-based prediction of LRH and CAI on Canadian gold ores. On the modelling side, the Vargas et al. (2025) benchmark on a copper porphyry SAG mill circuit shows what is achievable when integrated geometallurgical models combining JK Drop Weight Tests, BWi determinations, and SMC parameters are backed by enough laboratory testwork and operating data: mean relative deviations close to 1.5% in throughput prediction. The spatial-modelling toolkit available in the broader literature, hybrid geostatistics-ML approaches (Dutta & Emery, 2024), dual random fields (Riquelme, 2025), and ensemble Kalman filter updating (Mehrali, 2026) , gives operators several routes for folding these hardness predictions into resource block models. Executive Order 14241 and the 2025 List of Critical Minerals create clear incentives to adopt these advances, because the credibility of supply chain assessments under Nassar et al. (2025) ultimately rests on the accuracy of domestic production projections coming out of operator-level resource models. Worthwhile next steps would include systematic

validation of HSI-based hardness prediction on U.S. lithium pegmatite, REE carbonatite, and cobalt deposit types; standardised reporting protocols for proxy-derived BWi values; and federal data-sharing arrangements enabling cross-operator benchmarking.

STATEMENTS ON COMPLIANCE WITH ETHICAL STANDARDS

Acknowledgments

The author thanks the Department of Mining Engineering at Michigan Technological University for institutional support during the preparation of this review.

Disclosure of conflict of interest

The author declares no competing financial or personal interests.

Data Availability

No primary data was generated or analyzed. The numerical values plotted in Figure 1 are reproduced from Ghadernejad et al. (2026), https://doi.org/10.3390/min16010115 . The values plotted in Figure 2 are reproduced from Vargas et al. (2025), https://doi.org/10.3390/mining5030037 . The Mountain Pass operating performance values cited in Section 1 are reproduced from the USGS Mineral Commodity Summaries 2025, https://doi.org/10.3133/mcs2025 . All cited sources are publicly accessible.

REFERENCES

[1] Adidam, A. V. R., Mauerhofer, R., Aboubaker, M. G., Lehmann, B., & Spier, C. A. (2024). Identifying rare earth elements using a tripod and drone-mounted hyperspectral camera: A case study of the Mountain Pass Birthday Stock and Sulphide Queen Mine Pit, California. *Remote Sensing, 16*(17), 3353. https://doi.org/10.3390/rs16173353

[2] Adusei-Gyamfi, M., Akyea, B., & Awuah-Mensah, K. (2024). Uncertainty quantification in mineral resource estimation. *Natural Resources Research, 33*(5), 1817–1856. https://doi.org/10.1007/s11053-024-10394-6

[3] Davies, R. S., Trott, M., Georgi, J., & Farrar, A. (2025). Artificial intelligence and machine learning to enhance critical mineral deposit discovery. *Geosystems and Geoenvironment, 4*(2), 100361. https://doi.org/10.1016/j.geogeo.2025.100361

[4] Dutta, P. J., & Emery, X. (2024). Classifying rock types by geostatistics and random forests in tandem. *Machine Learning: Science and Technology, 5*(2), 025013. https://doi.org/10.1088/2632-2153/ad394e

[5] Fu, Z., Zheng, X., Yan, Y., Xu, X., Zhou, F., Li, X., Zhou, Q., & Mai, W. (2025). The evolution of machine learning in large-scale mineral prospectivity prediction: A decade of innovation (2016–2025). *Minerals, 15*(10), 1042. https://doi.org/10.3390/min15101042

[6] Ghadernejad, S., Abdolmaleki, M., & Esmaeili, K. (2026). A multi-proxy framework for predicting ore grindability: Insights from geomechanical and hyperspectral measurements. *Minerals, 16*(1), 115. https://doi.org/10.3390/min16010115

[7] Goodall, W. R., Reeves, R., & Anderson, K. (2025). A comparative study of machine learning and traditional techniques for grade prediction and grade-tonnage evaluation in a small VMS deposit [Thesis]. Virginia Polytechnic Institute and State University. https://hdl.handle.net/10919/126478

[8] Hoerger, S., & Dagdelen, K. (2025). Conditional simulation for stochastic production scheduling of open pit mines. In L. Azevedo, J. Narciso, A. Soares, M. J. Pereira, & J. A. Vargas-Guzmán (Eds.), *International Geostatistics Congress 2024: Quantitative Geology and Geostatistics, Vol. 20* (pp. 397–408). Springer. https://doi.org/10.1007/978-3-031-92870-3_34

[9] Jamshidi, A., & Sousa, L. (2024). Accuracy of point load index and Brazilian tensile strength in predicting the uniaxial compressive strength of the rocks: A comparative study. *Materials, 17*(20), 5081. https://doi.org/10.3390/ma17205081

[10] Kabemba, A. M., & Waters, K. E. (2025). Towards a dynamic optimisation of comminution circuit under geological uncertainties. *Processes, 13*(2), 443. https://doi.org/10.3390/pr13020443

[11] Mehrali, S. (2026). Real-time updating of geochemical and geometallurgical spatial models with multivariate ensemble Kalman filtering: Application to Gol Gohar iron deposit. *Minerals, 16*(2), 141. https://doi.org/10.3390/min16020141

[12] Nassar, N. T., Pineault, D., Allen, S. M., McCaffrey, D. M., Padilla, A. J., Brainard, J. L., Bayani, M., Shojaeddini, E., Ryter, J. W., Lincoln, S., & Alonso, E. (2025). Methodology and technical input for the 2025 U.S. List of Critical Minerals: Assessing the potential effects of mineral commodity supply chain disruptions on the U.S. economy. *U.S. Geological Survey Open-File Report 2025-1047*, 32 p. https://doi.org/10.3133/ofr20251047

[13] Nikolić, V., Medina Pierres, J., Sanchez Calvo, M., Menendez-Aguado, J. M., Trumić, Mil., Trumić, Maj., & Milošević, V. (2025). Proposal of a method for calculating the Bond Work Index for samples with non-standard feed particle size distribution. *Minerals, 15*(4), 358. https://doi.org/10.3390/min15040358

[14] Riquelme, Á. I. (2025). Dual random fields and their application to mineral potential mapping. *Mathematical Geosciences, 57*(5), 845–881. https://doi.org/10.1007/s11004-025-10195-4

[15] Sahoo, S. K., Tripathy, S. K., Nayak, A., Hembrom, K. C., Dey, S., Rath, R. K., & Mohanta, M. K. (2024). Beneficiation of lithium bearing pegmatite rock: A review. *Mineral Processing and Extractive Metallurgy Review, 45*(1), 1–27. https://doi.org/10.1080/08827508.2022.2117172

[16] Tadesse, B., Albijanic, B., Makuei, F., & Browner, R. (2024). Recent advances in flotation of spodumene: A review of reagent chemistry and surface properties. *Minerals Engineering, 215*, 108812. https://doi.org/10.1016/j.mineng.2024.108812

[17] U.S. Geological Survey. (2025a). Mineral commodity summaries 2025. U.S. Geological Survey, 212 p. https://doi.org/10.3133/mcs2025

[18] U.S. Geological Survey. (2025b). Final 2025 list of critical minerals. *Federal Register, 90*(214), 50494–50497. Document No. 2025-19813.

[19] Vargas, F., Pinedo, V., Quiroz, M., & Vásquez, F. (2025). Comparative analysis of throughput prediction models in SAG mill circuits: A geometallurgical approach. *Mining, 5*(3), 37. https://doi.org/10.3390/mining5030037

[20] Wang, R., Zhao, K., Liu, X., Yang, Y., Ren, H., Yu, X., Wei, Y., & Chen, S. (2025). Comprehensive utilization beneficiation process of lithium pegmatite ore: A pilot-scale study. *Minerals, 15*(11), 1138. https://doi.org/10.3390/min15111138

[21] Wang, X. (2024). Uncertainty quantification in geochemical mapping: A review and recommendations. *Geochemistry, Geophysics, Geosystems, 25*(3), e2023GC011301. https://doi.org/10.1029/2023GC011301

[22] White House. (2025). Executive Order 14241: Immediate measures to increase American mineral production. *Federal Register, 90*(57), 13673–13677. Document No. 2025-05212.

[23] Zhang, H., Cao, Y., Luo, Q., & Qi, W. (2025). Assessing point load strength in irregular phyllite via an equivalent area method. *PLOS ONE, 20*(5), e0321740. https://doi.org/10.1371/journal.pone.0321740